APPLICATION OF OPTIMAL POLYNOMIAL CONTROLLER TO A BENCHMARK PROBLEM

A.K. Agrawal*, J.N. Yang* and J.C. Wu**
Department of Civil & Environmental Engineering
University of California, Irvine, CA 92697

ABSTRACT

In this paper, we investigate the performance of optimal polynomial control for the vibration suppression of a benchmark problem; namely, the active tendon system. The optimal polynomial controller is a summation of polynomials of different orders, i.e., linear, cubic, quintic, etc., and the gain matrices for different parts of the controller are calculated easily by solving matrix Riccati and Lyapunov equations. A Kalman-Bucy estimator is designed for the on-line estimation of the states of the design model. Hence, the linear quadratic Gaussian (LQG) controller is a special case of the current polynomial controller in which the higher order parts are zero. While the percentage of reduction for displacement response quantities remains constant for the LQG controller, it increases with respect to the earthquake intensity for the polynomial controller. Consequently, if the earthquake intensity exceeds the design one, the polynomial controller is capable of achieving a higher reduction for the displacement response at the expense of control efforts. Such a property is desirable for the protection of civil engineering structures because of the inherent stochastic nature of the earthquake.

INTRODUCTION

Under strong earthquakes, the main objective of active control is to limit the peak response (e.g., displacement) of the structure to minimize the damage. However, it is difficult to obtain an optimal controller that minimizes the peak response of the structure.

---

* Graduate Research Assistant and Professor, respectively.

** Currently, Assistant Professor, Dept. of Civil Engg., Tamkang Univ., Taipei, Taiwan.

In this connection, it has been presented by Housner, Soong and Masri[1] that nonlinear controllers may be more effective than the classical linear controllers in reducing the peak response of linear structures. Such evidences were also observed elsewhere (e.g., Wu et al[2, 3], Tomasula et al[4, 5], Agrawal and Yang[6-9]). Wu et al[2, 3] and Tomasula et al[4, 5] have proposed a special polynomial controller for the peak response reduction of seismic-excited structures. They have shown advantages of the polynomial controller over the linear optimal controller for control of linear structures. The controller proposed by Wu et al[2, 3] is a special cubic order controller obtained by minimizing a nonquadratic performance index and it is similar to the cubic controller derived by Speyer[10]. Tomasula et al[4, 5] have proposed a polynomial controller using the tensor expansion method for a performance index that is quadratic in control and quartic in the states.

Recently, Agrawal and Yang[6-8] have presented a class of optimal polynomial controllers of various orders by minimizing a special performance index that is quadratic in control and polynomial of an arbitrary order of the states. This specific polynomial performance index belongs to a general class for which an exact optimal solution can be determined analytically. The resulting polynomial controller is a summation of polynomials of different orders, i.e., linear, cubic, quintic, etc., and the gain matrices for different parts of the controller are calculated easily from matrix Riccati and Lyapunov equations. This polynomial controller reduces to the controller presented by Wu et al[2, 3] for a specific choice of weighting matrices. Further, the optimal polynomial controller has been extended to the case of static output feedback by Agrawal and Yang[8, 9] as well as nonlinear and hysteretic structures[1, 11].

The objective of this paper is to investigate the performance of the optimal polynomial controller for a benchmark problem, i.e., the active tendon system. Since the state variables of the benchmark problem are not physical variables, the static output polynomial controller[8, 9] is not applicable. Hence, a Kalman-Bucy estimator is used for the on-line estimation of the states of the design model. Consequently, the linear quadratic Gaussian (LQG) controller is a special case of the current polynomial controller in which the higher order parts are zero. Numerical simulations have been conducted by designing various cases of linear and polynomial (cubic) controllers. By varying the peak

ground acceleration of the earthquake, the percentage of the peak response reduction by the linear controller (LQG) remains constant. However, the percentage of the peak displacement reduction by the polynomial controller increases with the increase of the peak ground acceleration. In particular, when the earthquake intensity exceeds the specified (design) one, the polynomial controller is capable of achieving a higher percentage of reduction for the peak displacement response; however at the expense of using larger control efforts. Such a load-adaptive property is very desirable for control of civil engineering structures because of the inherent stochastic nature of earthquakes. The advantage of this load adaptive property for the reduction of peak displacement responses of seismic excited structures is demonstrated by simulation results.

FORMULATION

Reduced-order model (design model)

A reduced-order model (design model) for the three-story structure equipped with an active tendon system has been derived from the evaluation model in Spencer et al[12, 13] using *balreal* and *modred* functions in MATLAB control system toolbox[14] as follows

$$\dot{x}_r = A_r x_r + B_r u + E_r \ddot{x}_g \tag{1}$$

$$y_r = C_{y_r} x_r + D_{y_r} u_r + F_{y_r} \ddot{x}_g + v \tag{2}$$

$$z_r = C_{zr} x_r + D_{zr} u + F_{zr} \ddot{x}_g \tag{3}$$

where x_r is the reduced-order state vector with a dimension $r = 12$, $\ddot{x}_g$ is the scalar ground acceleration, u is the scalar control input, $y_r = [x_p, \ddot{x}_{a1}, \ddot{x}_{a2}, \ddot{x}_{a3}, f, \ddot{x}_g]'$ is the output feedback vector of responses that can be measured directly, $z_r = [\ x_1, x_2, x_3, x_p, \dot{x}_1, \dot{x}_2, \dot{x}_3, \dot{x}_p, \ddot{x}_{a1}, \ddot{x}_{a2}, \ddot{x}_{a3}, f]'$ is the control output vector to be regulated. Here, x_i is the relative displacement of the ith floor with respect to the ground, $\ddot{x}_{ai}$ is the absolute acceleration of the ith floor, x_p is the displacement (stroke) of the actuator, f is the tendon force, v is a vector of measurement noises, and A_r, B_r, E_r, C_{yr}, D_{yr}, C_{zr}, D_{zr}, F_{yr} and F_{zr} are matrices and vectors of appropriate dimensions. Further, we have

the freedom to choose appropriate control output z_r and feedback output y_r based on our control objective and sensor installations.

Design of optimal polynomial controller

An optimal polynomial controller for the linear system, Eq.(1), was obtained by minimizing a polynomial performance index [Agrawal and Yang[6, 7]]

$$J = \int_0^\infty [x'_r Q x_r + u' R u + \sum_{i=2}^{K} (x'_r M_i x_r)^{i-1} (x'_r Q_i x_r) + \bar{h}(x_r)] dt \tag{4}$$

in which a prime indicates the transpose of a matrix or vector and

$$\bar{h}(x_r) = [\sum_{i=2}^{k} (x'_r M_i x_r)^{i-1} x'_r M_i] B R^{-1} B' [\sum_{i=2}^{K} (x'_r M_i x_r)^{i-1} M_i x_r] \tag{5}$$

In Eq.(4), Q and Q_i, $i = 2, 3..., k$, are positive semi-definite state weighting matrices, R is a positive scalar control weighting element, and M_i, $i = 2, 3, ..., k$ are positive-definite matrices. The first two terms in Eq.(4) are the classical quadratic terms, whereas the third term in summation is polynomial in x_r of different orders higher than the quadratic term. The last term $\bar{h}(x_r)$, Eq.(5), is added such that simple analytical solutions can be obtained. Weighting matrices Q, R and Q_i (i=2, 3,..., k) can be chosen arbitrarily to penalize selected quantities. However, the matrices M_i (i=2, 3,..., k) are implicit functions of the weighting matrices Q_i (i=2, 3,..., k), which will be given later.

Because of the particular identification method used for constructing the evaluation and design models, reduced-order states, x_r, are not the physical states of the structure. The control output vector z_r, Eq.(3), involves not only x_r but also the control u and the earthquake ground acceleration $\ddot{x}_g$. Due to the nonlinear nature of the controller, it is difficult to construct appropriate weighting matrices Q and Q_i (i=2, 3, .., k) for z_r. Hence, Q and Q_i are chosen by neglecting the contributions of u and $\ddot{x}_g$ in z_r as follows

$$Q = C'_{zr} Q_d C_{zr} \quad ; \quad Q_i = C'_{zr} Q_{di} C_{zr}, \; i = 2, 3, .., k \tag{6}$$

where Q_d and Q_{di} are (12x12) diagonal weighting matrices. Elements of weighting matrices Q_d and Q_{di} should be chosen by considering relative importance of the elements in z_r.

The performance index in Eq.(4) has been minimized by solving the Hamilton-Jacobi-Bellman equation. An optimal polynomial control law is obtained analytically [Agrawal & Yang[6, 7]] as

$$u(t) = -R^{-1}B_r'Px_r(t) - R^{-1}B' \sum_{i=2}^{K} (x_r'M_i x_r)^{i-1} M_i x_r \tag{7}$$

in which positive-definite gain matrices P and M_i's are obtained by solving algebraic Riccati and Lyapunov equations, respectively

$$PA + A'P - PBR^{-1}B'P + Q = 0 \tag{8}$$

$$M_i(A - BR^{-1}B'P) + (A - BR^{-1}B'P)'M_i + Q_i = 0, \quad \text{for } i = 2, 3, \ldots, k \tag{9}$$

The optimal polynomial controller in Eq.(7) consists of linear and nonlinear parts. The linear part is the same as that of the linear quadratic regulator (LQR), while the nonlinear part of the controller consists of odd-order multinomials in terms of the states x_r, i.e., cubic, quartic, quintic, etc. Matrices P and M_i's in Eqs.(8) and (9) can be solved using any well-known numerical algorithm or using functions available in MATLAB.

Kalman-Bucy Estimator for x_r

The implementation of the optimal polynomial controller in Eq.(7) requires the knowledge of the reduced-order vector x_r, which should be estimated from the measurement vector $y_r = [x_p, \ddot{x}_{a1}, \ddot{x}_{a2}, \ddot{x}_{a3}, f, \ddot{x}_g]'$. The Kalman-Bucy filter described in Spencer et al[12, 13] is given as follows

$$\dot{\hat{x}}_r = A_r \hat{x}_r + B_r u + L_o (y_r - C_{yr} \hat{x}_r - D_{yr} u) \tag{10}$$

in which $\hat{x}_r$ is the estimated state and L_o is the observer gain matrix. For on-line integration, the observer in Eq.(10) can be written as

$$\dot{\hat{x}}_r = (A_r - L_o C_{yr}) \hat{x}_r + (B_r - D_{yr})u + L_o y_r \tag{11}$$

Since the polynomial controller is nonlinear, the on-line implementation of the observer in Eq.(11) requires not only the measurement y_r but also the control command u. The observer in Eq.(11) was derived using the separation principle, which applies only to linear controllers. It has not been shown analytically that the observer in Eq.(11) can be used for the polynomial controller. Further, unlike linear controllers, the stability of the observer in Eq.(11) for nonlinear controllers can be investigated only through numerical simulation. Despite of the drawbacks above, we shall use the observer equation in Eq.(11) to investigate the performance of the polynomial controller.

The optimal controller in Eq.(7) includes the linear controller (first part) as a special case which is the LQG controller, when the observer in Eq.(11) is used. Consequently, the optimal polynomial controller investigated herein is more general than the LQG controller, and hence it provides the designer with more degrees of flexibility for different control objectives.

The stability of the polynomial controller in Eq.(7) has been proved in Agrawal and Yang[6, 7] and it can be shown that the system in Eq.(1) using the polynomial controller is asymptotically stable. For the benchmark problem in Eqs.(1) to (3), the reduced-order state vector x_r has to be estimated from the output measurements y_r using the Kalman-Bucy filter, Eq.(11). For the LQG controller, i.e., the linear part in Eq.(7) and the estimation of x_r (i.e., $\hat{x}_r$) from Eq.(11), the stability of the closed-loop system can be established based on the separation principle [e.g., Meirovitch[15]]. On the other hand, the stability of the closed-loop system for the polynomial controller in Eq.(7) using the estimation of x_r (i.e., $\hat{x}_r$) from Eq.(11) cannot be guaranteed, because the separation principle is not applicable. However, it has been found through the results of numerical simulations that the closed-loop system given by Eqs.(1), (7) and (11) is generally stable.

NUMERICAL SIMULATIONS

Numerical simulations were conducted using the MATLAB SIMULINK program for the evaluation model subject to the El Centro, Hachinohe and stochastic earthquakes, as described in Spencer et al[12, 13]. For the zeroed system, i.e., the system with the control command u(t)=0, the peak response quantities due to the El Centro and Hachinohe

earthquakes are shown in columns (2) and (3) of Table 1. The root-mean-square response quantities due to the stochastic earthquake are presented in column (5) of Table 1. Quantities in Table 1 will serve as the measure of the performance of the active tendon system.

With active control, the control output z_r is chosen to be $z_r = [\ d_1,\ d_2,\ d_3,\ x_p,\ \dot{x}_1,\ \dot{x}_2,\ \dot{x}_3,\ \dot{x}_p,\ \ddot{x}_{a1},\ \ddot{x}_{a2},\ \ddot{x}_{a3},\ f]'$ in which d_i indicates the ith interstory drift. We shall investigate only two controllers; namely, the linear controller (LQG), i.e., the first part in Eq.(7), and the cubic controller, i.e., the first part and the second part with k=2 in Eq.(7). For each controller, three different design cases are considered; namely, 5-sensor, 3-sensor and 1-sensor. The output feedback quantities for the three cases are as follows: (i) 5-sensor case; $y_r = [\ x_p,\ \ddot{x}_{a1},\ \ddot{x}_{a2},\ \ddot{x}_{a3},\ f]'$, (ii) 3-sensor case; $y_r = [\ \ddot{x}_{a1},\ \ddot{x}_{a2},\ \ddot{x}_{a3}]'$, and (iii) 1-sensor case; $y_r = \ddot{x}_{a3}$. For each of the design cases above, the states of the reduced-order system, x_r, are estimated from the Kalman-Bucy observer, Eq.(11). The observer gain L_o in Eq.(11) has been designed by choosing $S_{\ddot{x}_g\ddot{x}_g} = 0.5$ and $S_{vv} = I_m$, where I_m is the (mxm) identity matrix with m being the number of sensors [Spencer et al[12, 13]]. Fig.1 shows the SIMULINK model for the polynomial (cubic) controller with 5-sensor measurements. In Fig. 1, the term "linear gain" stands for the first part of the controller in Eq.(7), i.e., $R^{-1}B_r'P$, and the term "nonlinear gain" stands for the second part of the controller, $R^{-1}B_r'M_2$, where M_2 is obtained from Eq.(9) for k=2. Other blocks displayed in Fig. 1 are the same as that described in Spencer et al[13].

For the three linear controllers (LQG) described above, the control parameters are as follows: (i) 5-sensor case; Q_d=diag [1, 1, 1, 0, 0, 0, 0, 0, 1, 1, 1, 6], R=4.0, (ii) 3-sensor case; Q_d=diag [1, 1, 1, 0, 0, 0, 0, 0, 1, 1, 1, 8.5], R=10.0, and (iii) 1-sensor case; Q_d=diag [1, 1, 1, 0, 0, 0, 0, 0, 1, 1, 1, 8.5], R=2.5. For the three polynomial (cubic) controllers, the control parameters are chosen as follows: (i) 5-sensor case; Q_d=diag [1, 1, 1, 0, 0, 0, 0, 0, 1, 1, 1, 4], Q_{d2}=diag [1, 1, 1, 0, 0, 0, 0, 0, 1, 1, 1, 2], R=10.0, (ii) 3-sensor case; Q_d=diag [1, 1, 1, 0, 0, 0, 0, 0, 1, 1, 1, 1], Q_{d2}=diag [1, 1, 1, 0, 0, 0, 0, 0, 1, 1, 1, 1], R=10.0, and (iii) 1-sensor case; Q_d=diag [1, 1, 1, 0, 0, 0, 0, 0, 1, 1, 1, 6],

Q_{d2}=diag [1, 1, 1, 0, 0, 0, 0, 0, 1, 1, 1, 3.8], R=60.0. All the controllers above are first designed such that the control constraints, e.g., $\max_t |u(t)| \le 3$, $\max_t |x_p(t)| \le 3$ and $\max_t |f(t)| \le 12$, are satisfied for the El Centro earthquake. Then, further simulations are conducted using Hachinohe and stochastic earthquakes to verify whether all the control constraints are satisfied or not. The controller is redesigned using the El Centro earthquake, if any of the constraints is violated. All the controllers are designed to utilize as much as possible the capacity of the actuator (i.e., the control efforts) without violating the control constraints, i.e., $\max_t |u(t)| \le 3$, $\max_t |x_p(t)| \le 3$ and $\max_t |f(t)| \le 12$. Numerical simulations for all the controllers presented above are conducted by incorporating time-delays and measurement noise as specified in the benchmark problem using the SIMULINK modules in Fig. 1. In Fig. 1, the "Sensor Noise" block adds the specified noise to sensor measurements, the "Discrete Controller" implements the Kalman-Bucy filter with a sampling rate of 0.001 sec., and the "Unit Delay" block introduces the computational time-delay of 200 μ sec. Besides this, magnitudes of all the output measurements as well as the control signal u(t) have been limited to ± 3V using the two saturation blocks in Fig. 1.

Simulation results for the evaluation criteria J_1 to J_{10} of the evaluation model for the El Centro, Hachinohe and stochastic earthquakes are presented in Table 2. The root-mean-square control voltage under the stochastic earthquake is denoted by σ_u in Table 2, whereas the peak control voltage under El Centro and Hachinohe earthquakes are denoted by u_p in the table. For the stochastic earthquake, the results presented in Table 2 for the evaluation criteria J_1, ..., J_5 and σ_u are somewhat different from that specified in Spencer et al[13]. We did not vary the earthquake parameters ζ_g and ω_g, because it takes too much computer time to search. The results presented in Tables 1 and 2 correspond to the nominal values ζ_g=0.3, ω_g=14.5 rad/sec, and T_f=750 secs [Spencer et al[13]]. Further, for the deterministic earthquakes, i.e., El Centro and Hachinohe, we don't choose the maximum value for J_6, ..., J_{10} and u_p, but present all the results for each earthquake in Table 2.

For the 5-sensor case, evaluation criteria and other control quantities for linear and nonlinear controllers are presented in columns (2) and (3), respectively.

Comparing the evaluation criteria J_1 to J_{10} for the two controllers in Table 2, it is observed that the performance of the cubic controller is slightly worse than that of the linear controller for El Centro and Hachinohe earthquakes. The reasons will be explained later in the conclusion. For the stochastic earthquake, the responses for the cubic controller are slightly higher but the required control efforts are slightly smaller. For all the simulation results presented in Table 2, although all the constraints on the control efforts given in Spencer et al[13] are satisfied, the margins for some of the constraints are quite small since controllers are designed to use the control efforts as much as possible without a violation of constraints.

The control energy requirement at any time instant t can be calculated as

$$E_b(t) = \int_0^t \dot{x}_p \, f \, dt \tag{12}$$

For the El-Centro earthquake, the time-history plots of the control energy buildup for linear and cubic controllers for the 5-sensor case are presented in Fig. 2. It is observed from Fig. 2 that although the cubic controller requires higher peak control command as compared with the linear controller (Table 2), the total control energy requirement by the cubic controller is slightly smaller than that of the linear controller.

The results presented so far are obtained using earthquakes with specified intensities, e.g., the peak ground acceleration (PGA) for the El-Centro earthquake is 0.348g. Since the peak ground acceleration of earthquakes is stochastic in nature, simulations have been conducted for the 5-sensor case by varying the peak ground acceleration (PGA) of the El Centro earthquake from 0.2g to 1.0g. In this case, all the constraints, such as the peak voltage, have been removed for the PGA greater than 0.348g. Results of simulation for the same linear and cubic controllers above are presented in Figs. 3 to 7. Fig. 3 shows the reduction in percentage (%) of the peak floor displacement, max $|x_i(t)|$, as a function of PGA. As expected, the reduction percentage for the peak displacements for the linear controller remain constant. On the other hand, the reduction percentages for the peak displacement by the cubic controller increase with

the increase of PGA. It should be noted from Fig. 3 that the percentage of reduction for the first floor displacement is about the same for the linear and cubic controllers at the design PGA of 0.348g. It is further observed from Fig. 3 that (i) for PGA < 0.348g, the peak displacement reduction for the cubic controller is smaller than that for the linear controller, and (ii) for PGA > 0.348g, the peak displacement reduction for the cubic controller is higher than that of the linear controller. The latter behavior is very desirable, since a larger percentage of reduction for the peak displacement is needed when the actual earthquake intensity exceeds the design one. However, as will be shown in the following, such a higher percentage of reduction for the peak displacement is accompanied by the requirement of larger control efforts.

Fig. 4 shows the plots of the percentages of reduction for the peak floor absolute acceleration vs. PGA. As expected, the percentages of reduction for the peak floor acceleration remain constant for the linear controller. However, the results degrade slightly, in the range of $\pm 5\%$, for the cubic controller. Fig. 5 shows the plots of two evaluation criteria J_6^* and J_7^* defined by

$$J_6^* = \max_t \left\{ \frac{d_1}{x_{3o}}, \frac{d_2}{x_{3o}}, \frac{d_3}{x_{3o}} \right\}, \quad J_7^* = \max_t \left\{ \frac{\ddot{x}_{a1}}{\ddot{x}_{3o}}, \frac{\ddot{x}_{a2}}{\ddot{x}_{3o}}, \frac{\ddot{x}_{a3}}{\ddot{x}_{3o}} \right\} \tag{13}$$

for the El Centro earthquake. It is observed from Fig. 5 that while J_6^* and J_7^* remains constant for the linear controller, J_6^* decreases and J_7^* increases with respect to PGA for the cubic controller. Hence, for the cubic controller, the reduction for the peak interstory drift increases with PGA whereas the reduction of the peak floor acceleration reduces with PGA.

Fig. 6 shows the plots of normalized peak tendon force, f, and peak control signal, u, vs. PGA. These quantities have been normalized, respectively, by f = 29.867 kN and u= 6.967 volts, which are obtained for the linear controller with 1g El Centro earthquake. For the linear controller, the plots for f and u coincide with each other as expected and they are denoted by the solid curve. For the cubic controller, it is interesting to note that the peak tendon force is very close to that of the linear controller. Consequently, the control force requirements for the linear and cubic controllers are about the same.

Further, it is observed that the control signal u increases significantly with PGA for the cubic controller.

The normalized peak actuator stroke x_p and peak actuator velocity $\dot{x}_p$ vs. PGA are displayed in Fig. 7. These quantities have been normalized, respectively, by x_p = 0.859 cm and $\dot{x}_p$ = 16.734 cm/sec., which are obtained for the linear controller with 1g El Centro earthquake. In Fig. 7, the plots of normalized x_p and $\dot{x}_p$ coincide with each other for the linear controller as expected, and they are indicated by the solid curve. It is observed from Fig. 7 that, when the earthquake peak ground acceleration (PGA) exceeds the design one (i.e., 0.348g), the cubic controller requires actuators with a longer stroke and a bigger velocity than that required by the linear controller. Consequently, when the actual earthquake intensity exceeds that of the design earthquake (i.e., PGA > 0.348g), the nonlinear controller achieves a higher level of reduction for peak displacements than the linear controller but at the expense of requiring larger control efforts, including peak stroke and peak velocity of the actuator. Note that the linear controller can achieve the same percentage of displacement reduction as the nonlinear controller for earthquake larger than the design PGA (i.e., PGA > 0.348g) by using a higher gain. However, a higher gain will lead to the violation of the constraints on the control efforts (actuator capacity) at the design earthquake (i.e., PGA = 0.348g).

CONCLUSIONS

The performance of optimal polynomial controllers for the active tendon system of the benchmark problem has been investigated. A Kalman-Bucy estimator has been used for the on-line estimation of the states of the design model. The polynomial controller includes the LQG controller as a special case. Hence, it provides more degrees of flexibility for the designer to deal with particular control objectives. Numerical simulations have been conducted for various cases of linear and cubic order controllers, and the performances of linear and nonlinear controllers have been compared on the basis of the simulation results.

Based on the simulation results presented in this paper for a benchmark problem

and that presented in the literature [Refs. 2-7], the advantages of the polynomial controllers over linear controllers depend on the particular structure considered and the particular earthquake record used. For instance, it was found in Refs. 2-3 that the polynomial controller is more effective in limiting the peak response for the same level of peak control force. This situation was not observed in Refs. 3-7. It was found in Refs. 3-7 that for many earthquake records, the required control energy for polynomial controllers is smaller than that for linear controllers for the same level of peak response reduction. In particular, the nonlinear controller requires much smaller control energy than the linear controller for the Mexico earthquake [Refs. 6, 7]. For the particular benchmark problem considered in this paper, neither of the advantages above is observed. Rather, the performance of nonlinear controllers in some cases is slightly worse than that of linear controllers for the given design earthquake, i.e., PGA = 0.348g. The main reason is explained in the following.

Since the state variables in the reduced-order state vector, x_r, are not physical quantities, there is a difficulty to minimize the performance index in terms of the control output z_r, that is a function of the state vector x_r, control u and ground acceleration $\ddot{x}_g$, for nonlinear controllers. The approximation of the control output z_r by $C_{zr}x_r$ for nonlinear controllers in adjusting the weighting matrices in Eq.(6) makes the design of the polynomial controller more involved, i.e., requiring more trials for the weighting matrices, and there is no direct relation between the weighting element and the element of the control output z_r. This problem doesn't exist if either the state variables used for the structural model are physical quantities, such as those used in the literature [Refs. 2-7], or the controller is linear. Further, since the MATLAB SIMULINK program is used for simulations, the estimation of the state vector $\hat{x}_r$ for the polynomial controller requires longer computer time.

In comparison with the linear controller (LQG), despite of the drawback above, the polynomial controller has the capability of achieving a higher level of reduction for the peak displacement at the expense of larger control efforts (i.e., actuator stroke and velocity) if the earthquake intensity is bigger than the design one. This advantage is consistent with that observed in the literature [Refs. 5-7]. Simulation results demonstrate

that, for the cubic controller, the percentage of reduction for the peak displacement increases with respect to the earthquake intensity. This property is quite desirable for protecting civil engineering structures, since the earthquake intensity is stochastic in nature. Finally, the optimality of the polynomial controller presented in this paper is meaningful only after weighting matrices and the order of nonlinearity are defined, similar to the interpretation of the LQR controller.

ACKNOWLEDGMENT

This paper is supported by the National Science Foundation through Grant No. CMS-96-25616. The efforts of Dr. Erik A. Johnson, Visiting Research Assistant Professor, Civil Engineering and Geological Sciences, University of Notre Dame, in verifying the results presented in this paper are gratefully acknowledged.

REFERENCES

1. G.W. Housner, T.T. Soong and S.F. Masri, 'Second generation of active structural control in civil engineering', Proc. First World Conference on Structural Control, pp. panel 1-18, USC Publication, L.A., CA (1994).
2. Z. Wu, V. Gattulli, R.C. Lin and T.T. Soong, (1994), 'Implementable control laws for peak response reduction', Proceedings of the First World Conference on Structural Control, Pasadena, CA., August 1994, pp. TP250-TP259 (1994).
3. Z. Wu, R.C. Lin and T.T. Soong, 'Nonlinear feedback control for improved peak response reduction', *Smart Materials and Structures*, Vol. 4, No. 1, pp. 140-148 (1995).
4. D.P. Tomasula, B.F. Spencer, Jr. and M.K. Sain, 'Limiting extreme structural responses using an efficient nonlinear control law', Proceedings of the First World Conference on Structural Control, Pasadena, CA., August 1994, pp. FP422-FP431 (1994).
5. D.P. Tomasula, B.F. Spencer, Jr. and M.K. Sain, 'Limiting extreme structural responses using an efficient nonlinear control law', *Journal of Engineering Mechanics, ASCE*, Vol. 122, No. 3, pp. 218-229 (1996).
6. A.K. Agrawal and J.N. Yang, 'Optimal polynomial control for linear and nonlinear structures', Technical Report NCEER-95-0019, *National Center for Earthquake*

Engineering Research, State University of New York, , Buffalo (1995).

7. A.K. Agrawal and J.N. Yang, 'Optimal polynomial control for seismically excited linear structures', Journal of Engineering Mechanics, ASCE, Vol. 122, No. 8, pp. 753-761 (1996).
8. A.K. Agrawal and J.N. Yang, 'Optimal polynomial control for civil engineering structures using static output feedback', The Chinese Journal of Mechanics, Vol. 12, No. 1, pp. 91-102 (1996).
9. A.K. Agrawal and J.N. Yang,(1997), 'Static output polynomial control for linear structures', Journal of Engineering Mechanics, ASCE, Vol. 123, No. 6, pp. 639-643 (1997).
10. J.L. Speyer, 'A nonlinear control law for a stochastic infinite time-problem', IEEE Trans. on Automatic Control, AC-21, No. 4, pp. 560-564 (1976).
11. J.N. Yang, A.K. Agrawal and S. Chen, 'Optimal polynomial control for seismically excited nonlinear and hysteretic structures', Journal of Earthquake Engineering & Structural Dynamics, Vol. 25, No. 11, pp. 1211-1230 (1996).
12. B.F. Spencer, S.J. Dyke and H.S. Deoskar, 'Benchmark problems in structural control part i: active mass driver systems', Proc. 1997 ASCE Structures Congress, April 13-16, Portland, OR (1997).
13. B.F. Spencer, S.J. Dyke and H.S. Deoskar, 'Benchmark problems in structural control part ii : active tendon system', Proc. 1997 ASCE Structures Congress, April 13-16, Portland, OR (1997).
14. A. Grace, A.J. Laub, J.N. Little and C.M. Thompson, *Control System Toolbox User's Guide*, The Math Works Inc., MA (1992).
15. L. Meirovitch, *Dynamics and Control of Structures*, John Wiley & Sons Inc. New York, NY (1989).

Table 1 : Structural Response Quantities for the Zeroed System.

	El Centro			Hachinohe			Stochastic Earthquake			
(1) Quantities	(2) Story			(3) Story			(4) Quantities	(5) Story		
	1	*2*	*3*	*1*	*2*	*3*		*1*	*2*	*3*
x_i (cm)	2.03	4.97	6.57	1.19	2.95	3.85	σ_{x_i} (cm)	0.70	1.81	2.41
d_i (cm)	2.03	3.09	1.81	1.19	1.77	0.95	σ_{d_i} (cm)	0.70	1.11	0.60
$\ddot{x}_{ai}$ (g)	1.08	1.28	1.57	0.43	0.67	0.78	$\sigma_{\ddot{x}_{ai}}$ (g)	0.15	0.37	0.49
x_m (cm)	0.060			0.035			σ_{x_m} (cm)	0.020		
$\dot{x}_m$ (cm/s)	1.072			0.490			$\sigma_{\dot{x}_m}$ (cm/s)	0.291		
f (KN)	23.08			13.54			σ_f (KN)	7.90		

Table 2 : Comparison of evaluation criteria using linear and polynomial controllers for the Active Tendon System.

Quantities	Linear		Cubic	
Five-Sensor Case, $\mathbf{y}_r = [x_p, \ddot{x}_{a1}, \ddot{x}_{a2}, \ddot{x}_{a3}, f]'$				
(1)	(2)		(3)	
J_1	0.1562		0.1795	
J_2	0.3347		0.3850	
J_3	0.0314		0.0270	
J_4	0.0333		0.0289	
J_5	0.0092		0.0105	
σ_u (volts)	0.5845		0.5034	
σ_f (kN)	2.6533		3.0466	
σ_{x_p} (cm)	0.0735		0.0632	
	El Centro	Hachinohe	El Centro	Hachinohe
J_6	0.2380	0.3155	0.2251	0.3319
J_7	0.4869	0.8469	0.5119	0.8900
J_8	0.0464	0.0672	0.0547	0.0749
J_9	0.0584	0.0656	0.0757	0.0674
J_{10}	0.0360	0.0291	0.0373	0.0312
max $\lvert u \rvert$ (volts)	2.4287	2.0118	2.8633	2.2339
max $\lvert f \rvert$ (kN)	10.4081	8.4164	10.7772	9.0228
max $\lvert x_p \rvert$ (cm)	0.2994	0.2540	0.3526	0.2830
Three-Sensor Case, $\mathbf{y}_r = [\ddot{x}_{a1}, \ddot{x}_{a2}, \ddot{x}_{a3}]'$				
(4)	(5)		(6)	
J_1	0.1831		0.2136	
J_2	0.3920		0.4573	
J_3	0.0268		0.0227	
J_4	0.0283		0.0242	
J_5	0.0106		0.0124	
σ_u (volts)	0.4961		0.4215	
σ_f (kN)	3.0712		3.5969	
σ_{x_p} (cm)	0.0627		0.0532	
	El Centro	Hachinohe	El Centro	Hachinohe
J_6	0.2841	0.3335	0.2596	0.3549
J_7	0.5461	0.8716	0.5286	0.9123
J_8	0.0398	0.0472	0.0506	0.0490
J_9	0.0472	0.0503	0.0658	0.0498
J_{10}	0.0409	0.0296	0.0412	0.0320
max $\lvert u \rvert$ (volts)	2.0377	1.4157	2.5792	1.4641
max $\lvert f \rvert$ (kN)	11.8220	8.5672	11.9065	9.2366
max $\lvert x_p \rvert$ (cm)	0.2568	0.1785	0.3264	0.1851
One-Sensor Case, $\mathbf{y}_r = [\ddot{x}_{a3}]$				
(7)	(8)		(9)	
J_1	0.1374		0.1916	
J_2	0.2938		0.4111	
J_3	0.0380		0.0268	
J_4	0.0397		0.0285	
J_5	0.0081		0.0112	
σ_u (volts)	0.7049		0.4990	
σ_f (kN)	2.3276		3.2449	
σ_{x_p} (cm)	0.0888		0.0627	
	El Centro	Hachinohe	El Centro	Hachinohe
J_6	0.2137	0.3090	0.2349	0.3528
J_7	0.4879	0.8228	0.5022	0.8941
J_8	0.0570	0.0806	0.0585	0.0709
J_9	0.0657	0.0855	0.0741	0.0766
J_{10}	0.0343	0.0277	0.0397	0.0320
max $\lvert u \rvert$ (volts)	2.9243	2.4210	2.9289	2.1366
max $\lvert f \rvert$ (kN)	9.9068	8.0070	11.4668	9.2540
max $\lvert x_p \rvert$ (cm)	0.3675	0.3047	0.3771	0.2681

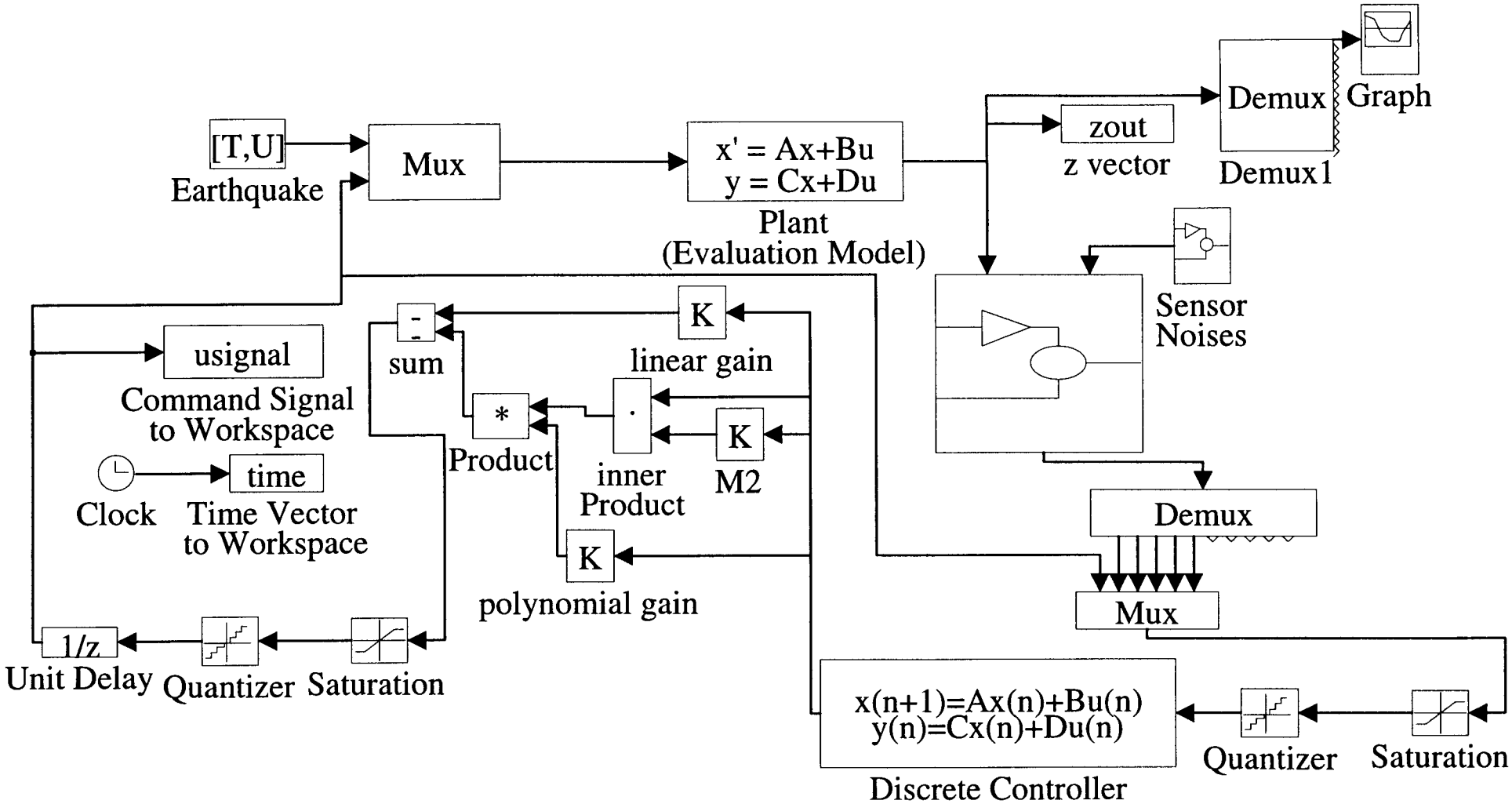

Fig. 1: Simulink block for polynomial controller with 5 sensors Using Deterministic Earthquake (El Centro or Hachinohe) Excitation.

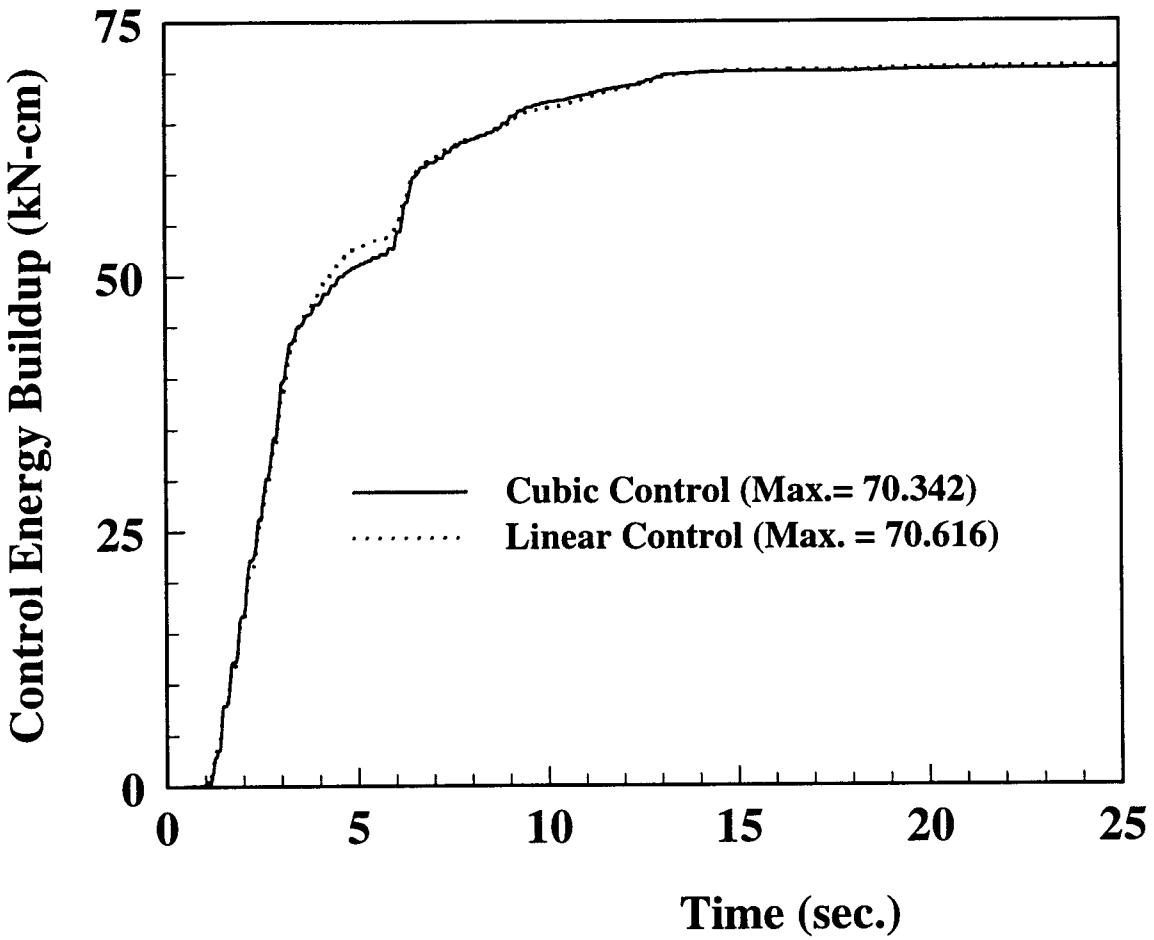

Fig. 2: Control energy buildup for linear and nonlinear controllers with 5 sensors for El Centro earthquake.

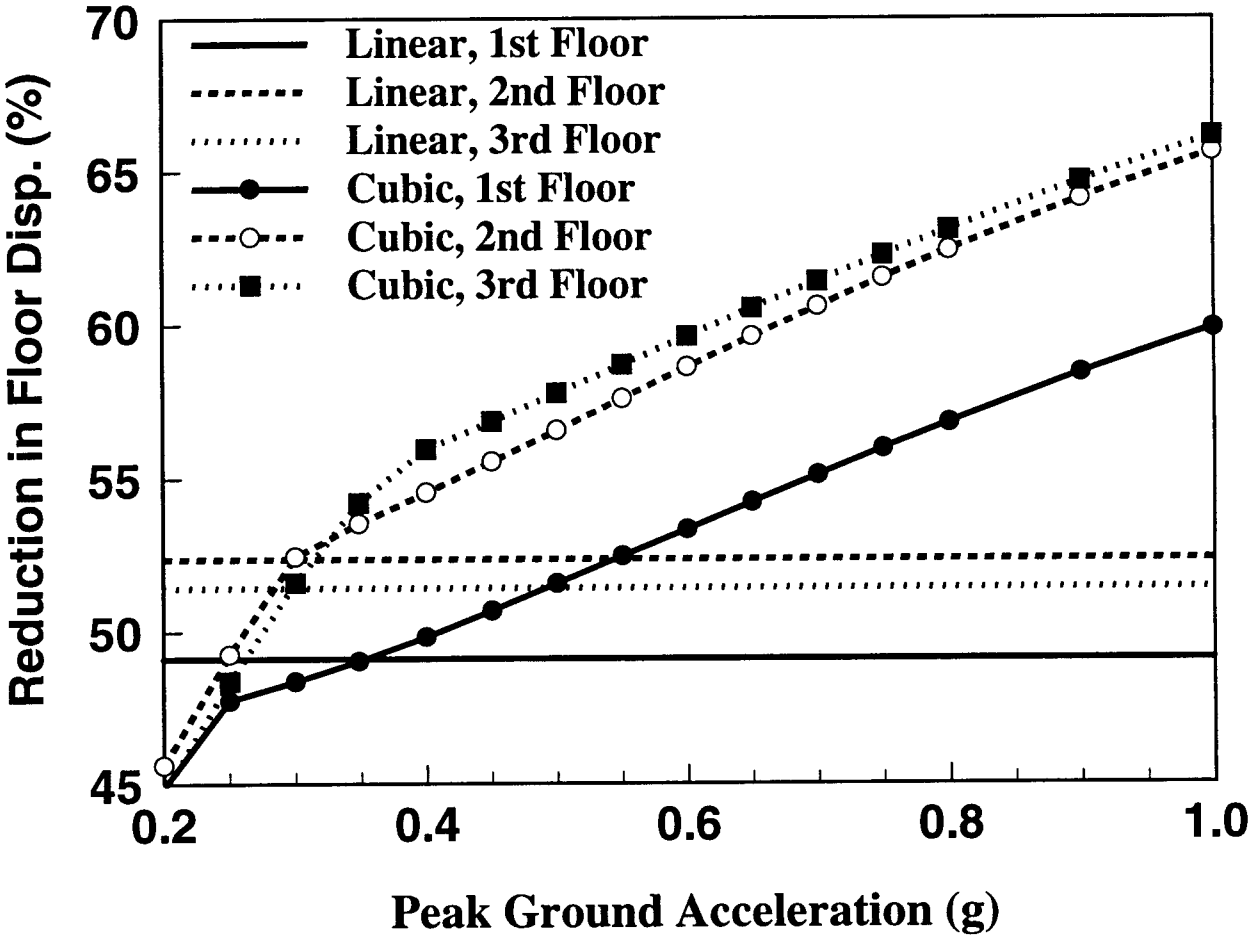

Fig. 3: Reduction in peak floor displacement vs. peak ground acceleration for El Centro earthquake.

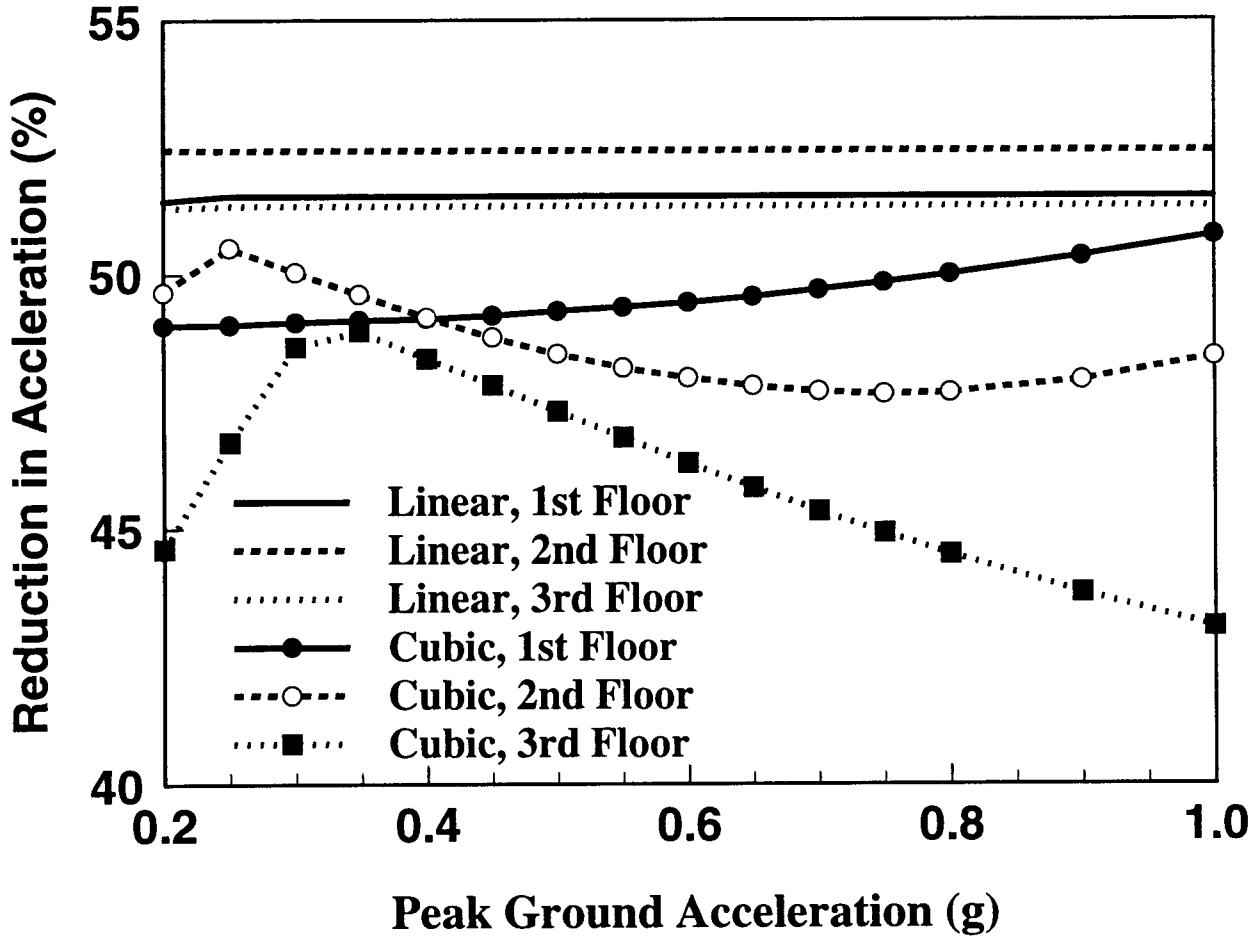

Fig. 4: Reduction in peak floor acceleration vs. peak ground acceleration for El Centro earthquake.

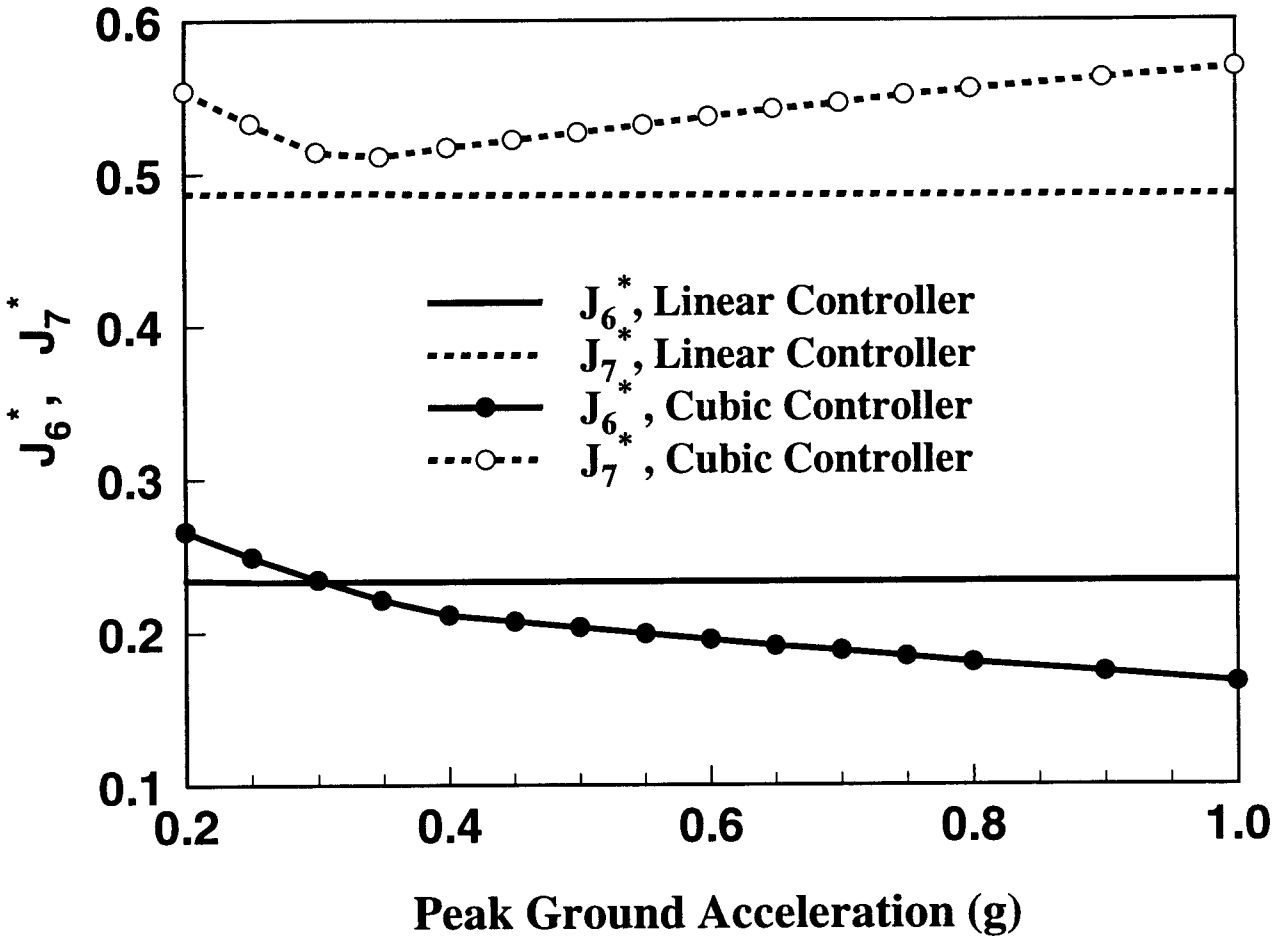

Fig. 5: Evaluation indices J_6^* and J_7^* vs. peak ground acceleration for El Centro earthquake.

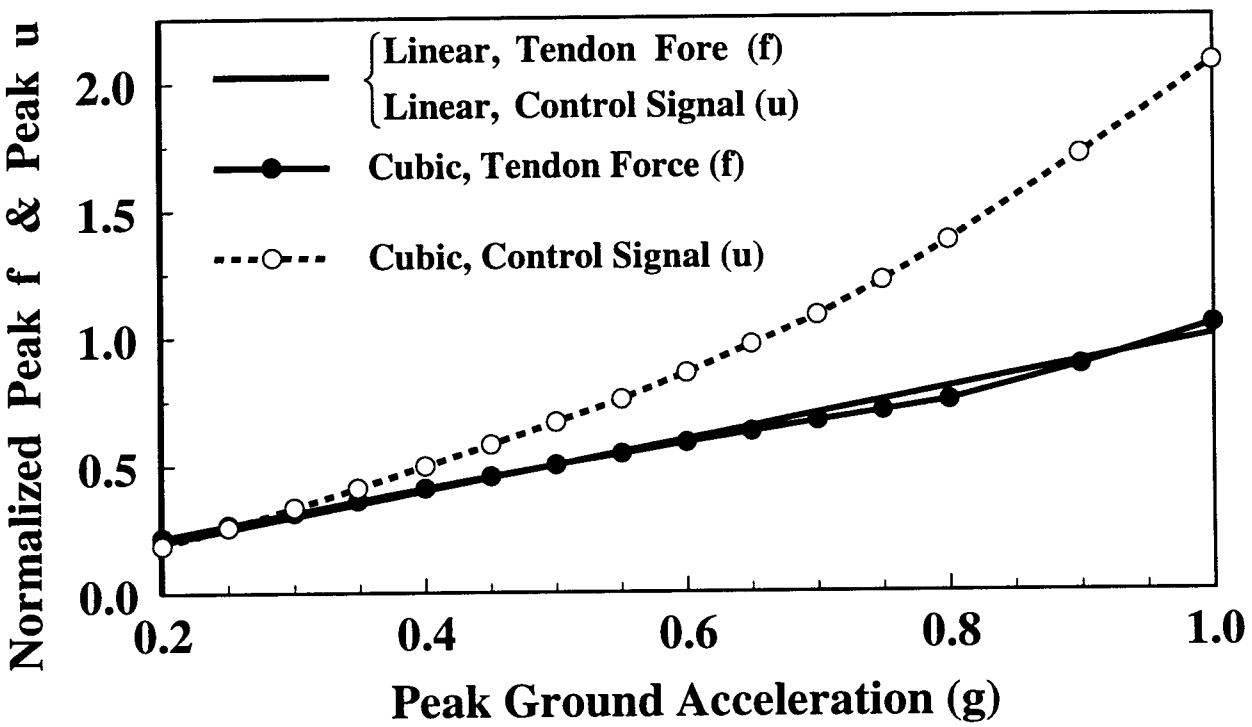

Fig. 6: Normalized peak tendon force f and peak control signal u vs. peak ground acceleration.

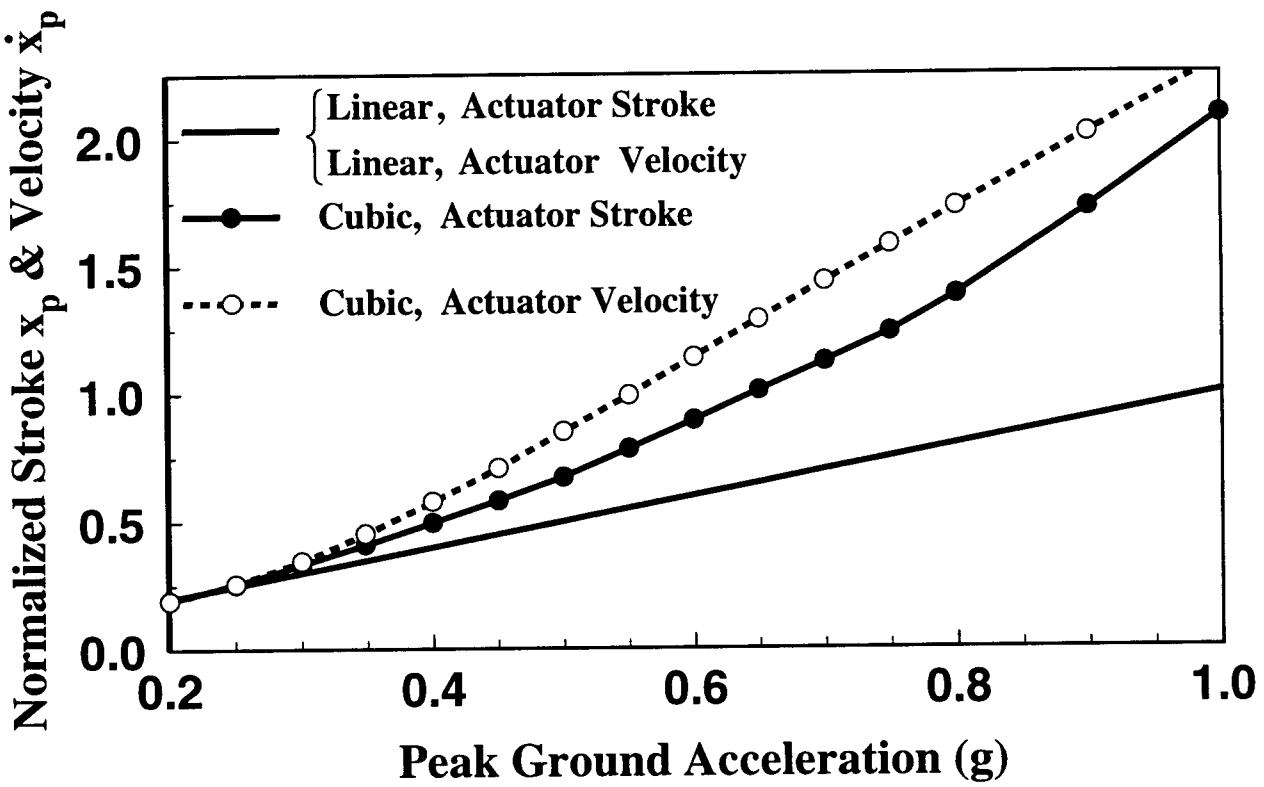

Fig. 7: Normalized actuator stroke and actuator velocity vs. peak ground acceleration.